Manganese-Mediated Oxidative Damage of Cellular and Isolated DNA by Isoniazid and Related Hydrazines: Non-Fenton-Type Hydroxyl Radical Formation†

Kimiko Ito, Koji Yamamoto, and Shosuke Kawanishi*

Department of Public Health, Faculty of Medicine, Kyoto University, Kyoto 606, Japan

Received May 20, 1992; Revised Manuscript Received August 25, 1992

ABSTRACT: The mechanism by which hydrazines induce damage to cellular and isolated DNA in the presence of metal ions has been investigated by pulsed-field gel electrophoresis (PFGE), DNA sequencing methods, and the ESR spin-trapping technique. For the detection of single-strand breaks by PFGE, an experimental procedure with alkali treatment has been designed. Isoniazid, hydrazine, and phenylhydrazine induced DNA single- and double-strand breaks in cells pretreated with Mn(II), whereas iproniazid did not. With isolated ^{32}P-DNA, isoniazid produced DNA damage in the presence of Cu(II), Mn(II), or Mn(III). Iproniazid damaged isolated DNA only in the presence of Cu(II). The Cu(II)-mediated DNA damage by isoniazid or iproniazid is due to active oxygen species other than hydroxyl free radical (•OH), presumably the Cu(I)–peroxide complex. Cleavage of isolated DNA by isoniazid plus Mn(II) occurred without marked site specificity. The DNA damage was inhibited by •OH scavengers and superoxide dismutase (SOD) but not by catalase, suggesting the involvement of •OH formed via O_2^- but not via H_2O_2. Consistently, in ESR experiments •OH formation was observed during Mn(II)-catalyzed autoxidation of isoniazid, and the •OH formation was inhibited by SOD, but not by catalase. Iproniazid plus Mn(II) produced no or little •OH. We propose a reaction mechanism for the •OH formation without a H_2O_2 intermediate during manganese-catalyzed autoxidation of hydrazine. The present and previous data raise the possibility that hydrazines plus Mn(II)-induced cellular DNA damage may occur, at least in part, through the non-Fenton-type reaction.

DNA damage by active oxygen species has drawn much interest in relation to carcinogenesis (Shibutani et al., 1991). Metal ions react with superoxide anion radical (O_2^-)[1] and H_2O_2 to produce more reactive oxygen species such as metal–oxygen complexes and hydroxyl free radical (•OH) in biological systems. The Fenton reaction of Fe(II) with H_2O_2 is an important mechanism for the generation of •OH and/or the ferryl ion (Inoue & Kawanishi, 1987; Loeb et al., 1988; Gutteridge et al., 1990; Stadtman & Berlett, 1991; Yamazaki & Piette, 1991). Several papers have suggested that DNA damage was caused by H_2O_2 through Fenton reaction in vivo (Imlay et al., 1988; Halliwell & Aruoma, 1991; Mello-Filho & Meneghini, 1991). Other metal ions such as Cu(II), Co(II), Mn(II), V(V), and Ni(II) have been shown to catalyze the formation of •OH, singlet oxygen, and/or metal–oxygen complexes from H_2O_2 (Inoue & Kawanishi, 1989; Yamamoto & Kawanishi, 1989; Yamamoto et al., 1989; Yim et al., 1990; Liochev & Fridovich, 1991; Tkeshelashvili et al., 1991; Hanna et al., 1992). However, whether these metal-mediated reactions may occur in vivo is still unclear.

Hydrazine derivatives have been implicated as mutagens and carcinogens (Toth, 1975; Parodi et al., 1981). However, little is known about the molecular mechanism of hydrazine-induced DNA damage. Isoniazid (isonicotinic acid hydrazide), an antituberculosis drug, has been shown to produce lung tumor in mice (Toth & Shubik, 1966; Severi & Biancifiori, 1968; Maru & Bhide, 1982) and to induce chromosome aberrations and sister chromatid exchanges in cultured rodent cells (MacRae & Stich, 1979). Isoniazid also induces mutation in bacteria without microsomal activation (Bhide et al., 1981; Wade et al., 1981; Braun et al., 1984). It is, therefore, considered that isoniazid induces DNA damage either directly or through mechanisms other than a drug-metabolizing enzyme system. It was shown that transition metals enhanced unscheduled DNA synthesis and chromosome aberrations induced by isoniazid in cultured cells (Whiting et al., 1979, 1980; Zetterberg & Boström, 1981). We have recently found that hydrazine and methylhydrazines generate •OH and other active species in the presence of metal ions (Kawanishi & Yamamoto, 1991; Yamamoto & Kawanishi, 1991a). These results let us consider the possibility that isoniazid could be activated by endogenous and/or exogenous metals to produce active oxygen species causing DNA damage in vivo.

In recent years, pulsed-field gel electrophoresis (PFGE) has emerged as a powerful tool for the study of high-molecular weight DNA. PFGE is generally used for detection of cellular DNA double-strand breaks (Blöcher et al., 1989). In addition, we have designed an experimental protocol which allows the detection of DNA single-strand breaks plus alkali-labile sites by PFGE. In this study, we have investigated damage to cellular and isolated DNA by isoniazid in the presence of metal ions using both PFGE and DNA sequencing technique. Active species causing DNA damage were investigated by the ESR spin-trapping method. The results are compared with those regarding iproniazid (isonicotinic acid 2-isopropylhy-

† This work was supported by a research grant from the Fujiwara Foundation of Kyoto University, a Grand-in-Aid for Cancer Research from Ministry of Health and Welfare, and Grants-in-Aid for Scientific Research from the Ministry of Education, Science and Culture of Japan.

* To whom correspondence and reprints requests should be addressed.

[1] Abbreviations: O_2^-, superoxide anion radical; •OH, hydroxyl free radical; PFGE, pulsed-field gel electrophoresis; SOD, superoxide dismutase; DTPA, diethylenetriaminepentaacetic acid; POBN, α-(1-oxy-4-pyridyl)-*N*-*tert*-butylnitrone; DMPO, 5,5-dimethyl-1-pyrroline *N*-oxide; DMPO–OH, hydroxyl radical adduct of 5,5-dimethyl-1-pyrroline *N*-oxide; FCS, fetal calf serum.

0006-2960/92/0431-11606$03.00/0

drazide), which is structurally similar to isoniazid, and other hydrazines to clarify the mechanism of hydrazine-induced DNA damage in vivo.

MATERIALS AND METHODS

Materials. Isoniazid and POBN were purchased from Aldrich. Iproniazid, SOD (3000 units/mg from bovine erythrocytes), and catalase (45 000 units/mg from bovine liver) were from Sigma. DMPO was from Labotec, Co. Ltd., Tokyo, Japan. Proteinase K was from Nacalai Tesque, Inc., Kyoto, Japan. DTPA and bathocuproinedisulfonic acid were from Dojin Chemicals Co., Kumamoto, Japan. [γ-^{32}P]ATP (6000 Ci/mmol) was purchased from Du Pont–New England Nuclear. Restriction enzymes (*Ava*I, *Xba*I, *Pst*I) and T_4 polynucleotide kinase were purchased from New England Biolabs, and *Not*I was from Takara Shuzo Co. Ltd., Kyoto, Japan. Peroxidase (260 units/mg from horseradish) was from Toyobo Co., Osaka, Japan. Mn(III)–pyrophosphate was prepared according to the procedure of Archibald and Fridovich (1982).

Detection of Cellular DNA Damage by Pulsed-Field Gel Electrophoresis. Raji cells (B lymphoblasts) were grown in RPMI 1640 (Gibco Laboratories, NY) supplemented with 7% FCS (Flow Laboratories, Inc., VA). For the determination of DNA double-strand breaks, cells (10^6 cells/mL) were incubated in RPMI 1640 containing 2% FCS at 37 °C for 2 h with or without addition of 100 μM $MnCl_2$ plus 1 mM glycine. Then the cells were harvested, washed once, and exposed to hydrazines freshly dissolved in RPMI 1640 plus 2% FCS at 37 °C for 3 h. The cells were washed three times with ice-cold PBS and resuspended in 300 μL of PBS. The cell suspension was mixed with an equal volume of 1.3% low-melting-point agarose, poured into sample holders, and allowed to harden at 4 °C for 30 min. Upon solidification, the agarose plugs were transferred to 1 mL of Tris/EDTA/2-mercaptoethanol buffer (0.5 M EDTA, 0.01 M Tris, 7.5% 2-mercaptoethanol) and incubated at 37 °C overnight, followed by incubation in 1 mL of NDS buffer (0.5 M EDTA, 0.01 M Tris, 1% *N*-laurylsarcosine, 1 mg/mL proteinase K) at 50 °C for 24 h. Electrophoresis was performed in 0.5 × TBE buffer (45 mM Tris, 45 mM boric acid, 1.25 mM EDTA, pH 8.3) by pulsed-field (CHEF-DRII DNA megabase electrophoresis system, Bio-Rad) at 200 V at 14 °C. Switch time was 60 s for 15 h followed by a 90-s switch time for 9 h. The DNA in the gel was visualized in ethidium bromide with a NTM-20 transilluminator (302 nm, 90 W; UVP, Inc., CA). For the detection of DNA single-strand breakage, the double-stranded DNA in the agarose plug was treated in 1 mL of 25 mM NaOH/2 mM EDTA (pH 12.5) at 4 °C for 90 min in the dark, neutralized, and electrophoresed by pulsed-field.

Analysis of Damage to Isolated DNA. DNA fragments were prepared from plasmid pbcNI which carries a 6.6-kilobase *Bam*HI chromosomal DNA segment containing human c-Ha-*ras*-1 protooncogene (Capon et al., 1983). Singly labeled 261-base-pair fragment (*Ava*I* 1645–*Xba*I 1905), 341-base-pair fragment (*Xba*I 1906–*Ava*I* 2246), 98-base-pair fragment (*Ava*I* 2247–*Pst*I 2344), and 337-base-pair fragment (*Pst*I 2345–*Ava*I* 2681) were obtained (Yamamoto & Kawanishi, 1989). The asterisk indicates ^{32}P-labeling, and nucleotide numbering starts with the *Bam*HI site.

The standard reaction mixture in a microtube (Eppendorf) contained 0.5 mM isoniazid, 20 μM metal ion, 20 μM sonicated calf thymus DNA (total nucleotide concentration), and ^{32}P-DNA fragment in 200 μL of 10 mM sodium phosphate buffer (pH 7.9) containing 5 μM DTPA. Since buffers and reagents are known to be invariably contaminated with trace amounts of metal ions, DTPA was added. After incubation at 37 °C for the indicated durations, the DNA fragments were heated at 90 °C in 1 M piperidine where indicated and electrophoresed as previously described (Yamamoto & Kawanishi, 1989).

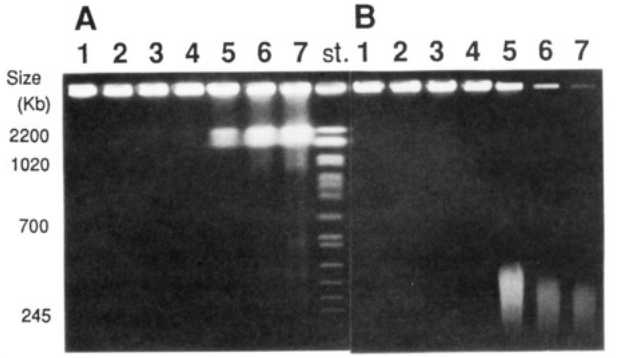

FIGURE 1: Detection of isoniazid plus Mn(II)-induced cellular DNA damage by PFGE. Raji cells were pretreated with glycine complex of 100 μM $MnCl_2$ for 2 h and then incubated with various concentrations of isoniazid for 3 h. The cells were prepared into agarose plugs, lysed, and subjected to PFGE through a 1% agarose gel, as described under Materials and Methods. The gel was stained in ethidium bromide. For detection of single-strand breaks, DNA in the agarose plug was denatured in dilute alkali. (A) Without alkali treatment; (B) with alkali treatment. Lane "st.", size marker DNA (*Saccharomyces cerevisiae*); lane 1, no treatment; lane 2, Mn(II); lane 3, Mn(II) + 0.05 mM isoniazid; lane 4, Mn(II) + 0.1 mM isoniazid; lane 5, Mn(II) + 0.2 mM isoniazid; lane 6, Mn(II) + 0.5 mM isoniazid; lane 7, Mn(II) + 1.0 mM isoniazid.

The preferred cleavage sites were determined by direct comparison of the positions of the oligonucleotides with those produced by the procedure of Maxam and Gilbert (1980) using a DNA sequencing system (LKB 2010 Macrophor). A laser densitometer (LKB 2222 UltroScan XL) was used for the measurement of the relative amounts of oligonucleotides from treated DNA fragments.

ESR Spectra Measurements. DMPO and POBN were used as radical trapping reagents. ESR spectra were measured at room temperature using a JES-FE-3XG (JEOL, Tokyo, Japan) spectrometer with 100-kHz field modulation (Kawanishi & Yamamoto, 1991). Spectra were recorded with a microwave power of 16 mW and a modulation amplitude of 1.0 G.

Measurement of Oxygen Consumption. The O_2 consumption during the autoxidation of hydrazines was measured in a thermostated (37 °C) water-jacketed glass vessel, fitted with a Clark electrode (Gilson, Paris, France) as reported previously (Kawanishi & Yamamoto, 1991).

RESULTS

Hydrazine-Induced DNA Damage in Cells Pretreated with Mn(II). In cells pretreated with Mn(II), isoniazid induced DNA double-strand breaks (Figure 1A). DNA fragments corresponding to 1–2 megabases were observed slightly at 0.05 mM and clearly at concentrations greater than 0.2 mM. Neither cells without pretreatment of Mn(II) nor cells with pretreatment of Cu(II) produced DNA strand breaks. Mn(II) alone did not produce the strand breaks (data not shown). We also analyzed single-strand breaks plus alkali-labile sites by PFGE after treating the double-stranded chromosome-sized DNA in agarose plug with dilute alkali. Figure 1B shows that, in DNA of the cells treated with isoniazid plus Mn(II), the peak of fragmented DNA molecule migrated further from the origin, suggesting the reduction of the DNA size with alkali. Under the experimental conditions employed,

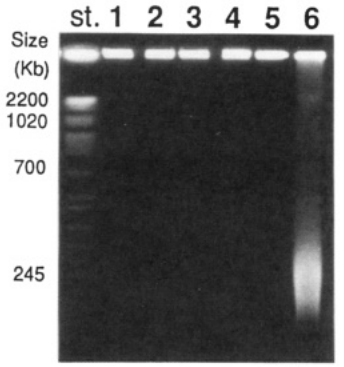

FIGURE 2: Detection of iproniazid or hydrazine-induced DNA single-strand breaks in cells pretreated with Mn(II). The DNA damage was analyzed by the method described in the Figure 1 legend. Lane "st.", size marker DNA (*S. cerevisiae*); lane 1, no treatment; lane 2, 1 mM iproniazid; lane 3, 100 μM Mn(II) + 1 mM iproniazid; lane 4, 0.5 mM hydrazine; lane 5, 100 μM Mn(II) + 0.1 mM hydrazine; lane 6, 100 μM Mn(II) + 0.5 mM hydrazine.

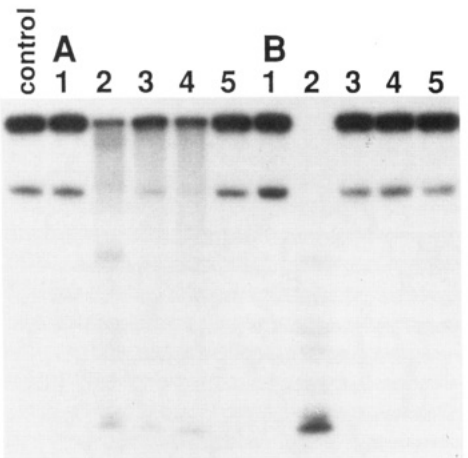

FIGURE 3: Autoradiogram of ^{32}P-labeled DNA fragments incubated with isoniazid or iproniazid in the presence of metal ions. The reaction mixture contained the ^{32}P-5′-end-labeled 337-base-pair fragment, 20 μM sonicated calf thymus DNA (total nucleotide concentration), and 5 μM DTPA in 200 μL of 10 mM sodium phosphate buffer at pH 7.9. Where indicated, 0.5 mM isoniazid (or iproniazid) and 20 μM metal ion were added. After the incubation at 37 °C for 30 min, followed by the piperidine treatment, the DNA fragments were electrophoresed on an 8% polyacrylamide, 8 M urea gel (12 × 16 cm), and the autoradiogram was obtained by exposing X-ray film to the gel. (A) Isoniazid was added; (B) iproniazid was added. Lane 1, no metal; lane 2, $CuCl_2$; lane 3, $MnCl_2$; lane 4, Mn(III)–pyrophosphate; lane 5, $(NH_4)_2Fe(SO_4)_2$.

control DNA produced no or little strand breaks even with the alkali treatment (Figure 1B, lane 1). Moreover, the alkali treatment did not increase the extent of DNA fragmentation induced by a restriction endonuclease recognizing an 8-base-pair sequence (*Not*I), which hydrolyzes the double-stranded DNA but causes neither single-strand breaks nor alkali-labile regions (data not shown). These results indicate that isoniazid induces single-strand breaks plus alkali-labile sites in DNA of the cells pretreated with Mn(II). The extent of DNA single-strand breaks induced by isoniazid plus Mn(II) was not reduced by catalase added extracellularly (data not shown). Hydrazine (Figure 2, lane 6) and phenylhydrazine (data not shown) also produced DNA single-strand breaks in cells pretreated with Mn(II). In contrast, iproniazid did not cause DNA strand breaks over a concentration range of 0.1–5 mM even in cells pretreated with Mn(II) (Figure 2, lane 3).

Cleavage of ^{32}P-Labeled DNA Fragments Induced by Isoniazid or Iproniazid in the Presence of Metal Ions or Peroxidase. The extent of damage to isolated DNA induced

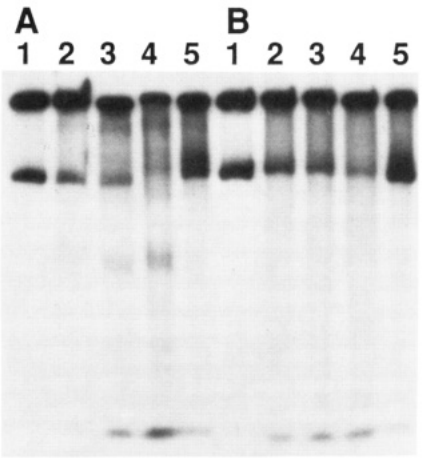

FIGURE 4: Time course of DNA cleavage induced by isoniazid in the presence of Cu(II) or Mn(II). The reaction mixture contained the ^{32}P-5′-end-labeled 337-base-pair fragment, 20 μM sonicated calf thymus DNA (total nucleotide concentration), 0.5 mM isoniazid, 20 μM metal ion, and 5 μM DTPA in 200 μL of 10 mM sodium phosphate buffer at pH 7.9. After the incubation at 37 °C for the indicated durations, followed by the piperidine treatment (lanes 1–4), or without the piperidine treatment (lane 5), the DNA fragments were analyzed by the method described in the Figure 3 legend. (A) $CuCl_2$ was added; (B) $MnCl_2$ was added. Lane 2, 10 min; lane 3, 20 min; lane 4, 30 min; lane 5, 30 min. Lane 1, incubation time was 30 min without isoniazid.

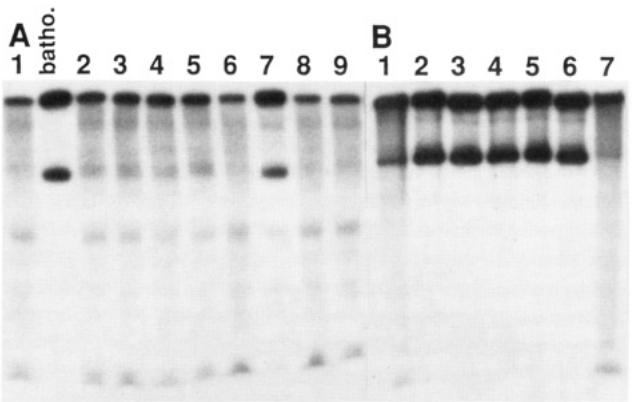

FIGURE 5: Effects of hydroxyl radical scavengers, SOD, and catalase on DNA cleavage induced by isoniazid in the presence of Cu(II) or Mn(II). The reaction mixture contained the ^{32}P-5′-end-labeled 337-base-pair fragment, 20 μM sonicated calf thymus DNA (total nucleotide concentration), 0.5 mM isoniazid, 20 μM metal ion, scavenger, and 5 μM DTPA in 200 μL of 10 mM sodium phosphate buffer at pH 7.9. After the incubation at 37 °C for 30 min, followed by the piperidine treatment, the DNA fragments were analyzed by the method described in the Figure 3 legend. (A) $CuCl_2$ was added; (B) $MnCl_2$ was added. Lane 1, no scavenger; lane 2, 0.8 M ethanol; lane 3, 0.2 M mannitol; lane 4, 0.2 M sodium formate; lane 5, 0.8 M dimethyl sulfoxide; lane 6, SOD (30 units); lane 7, catalase (30 units); lane 8, heat-denatured SOD (30 units); lane 9, heat-denatured catalase (30 units); lane "batho.", 50 μM bathocuproine.

by isoniazid in the presence of metal ions was estimated by gel electrophoretic analysis (Figure 3A). The upper band and lower band in the control show single-stranded and double-stranded forms of intact DNA fragment, respectively. Isoniazid alone caused no DNA damage (lane 1), showing that isoniazid itself is not a DNA-damaging agent. Isoniazid induced DNA damage in the presence of Cu(II) (lane 2), Mn(II) (lane 3), and Mn(III) (lane 4). No or little DNA damage was observed in the presence of Fe(II) (lane 5), Fe(III), Fe(III)–EDTA, or hemin (data not shown) under the present conditions. Metal ion alone induced no DNA damage. The order of ability to induce DNA damage with isoniazid was Cu(II) > Mn(II) ~ Mn(III) ≫ Fe(II) ~ Fe(III) ~

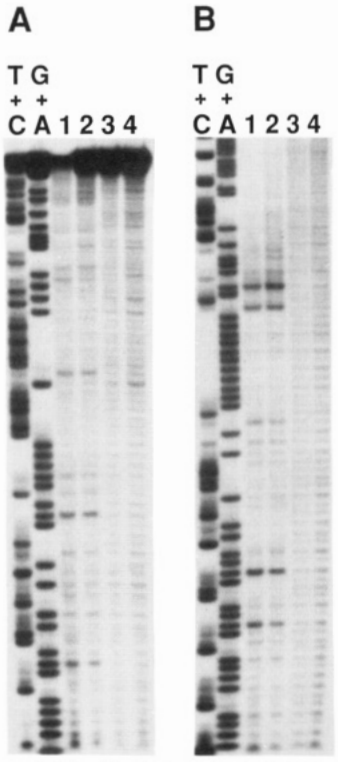

FIGURE 6: Site specificity of metal-mediated DNA cleavage induced by isoniazid or iproniazid. The ^{32}P-5′-end-labeled fragment in 200 μL of 10 mM sodium phosphate buffer at pH 7.9 containing 5 μM DTPA and 20 μM sonicated calf thymus DNA (total nucleotide concentration) was incubated with 0.5 mM iproniazid plus 20 μM $CuCl_2$, or with 0.5 mM isoniazid in the presence of 20 μM $CuCl_2$, $MnCl_2$, or Mn(III)–pyrophosphate at 37 °C for 30 min. After the piperidine treatment, DNA fragments were electrophoresed on an 8% polyacrylamide, 8 M urea gel using a DNA-sequencing system, and the autoradiogram was obtained by exposing X-ray film to the gel. The lanes G + A and T + C represent the patterns obtained for the same fragment after cleavage by the chemical methods of Maxam and Gilbert (1980). (A) The ^{32}P-5′-end-labeled 98-base-pair fragment (*Ava*I* 2247–*Pst*I 2344) was used. (B) The ^{32}P-5′-end-labeled 337-base-pair fragment (*Pst*I 2345–*Ava*I* 2681) was used. Lane 1, iproniazid + $CuCl_2$; lane 2, isoniazid + $CuCl_2$; lane 3, isoniazid + $MnCl_2$; lane 4, isoniazid + Mn(III)–pyrophosphate.

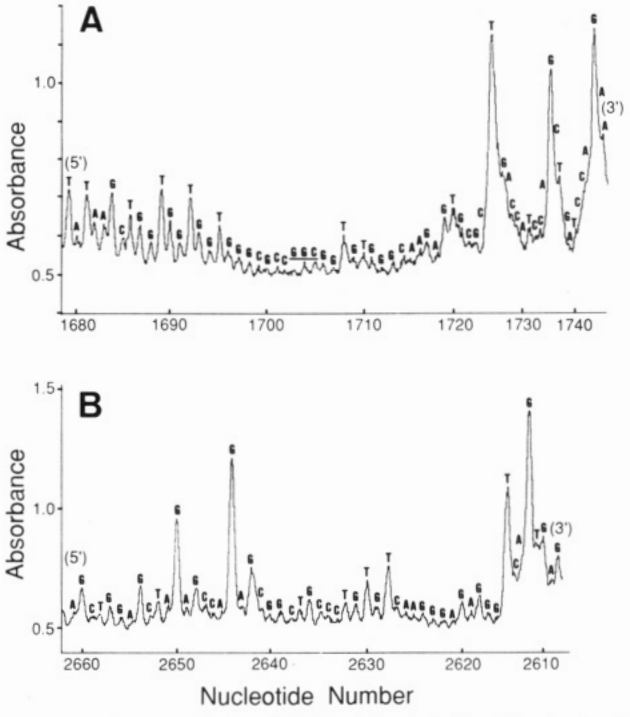

FIGURE 7: Site specificity of DNA cleavage induced by isoniazid plus Cu(II). (A) The ^{32}P-5′-end-labeled 261-base-pair fragment (*Ava*I* 1645–*Xba*I 1905) in 200 μL of 10 mM sodium phosphate buffer at pH 7.9 containing 5 μM DTPA and 20 μM sonicated calf thymus DNA (total nucleotide concentration) was incubated with 0.5 mM isoniazid plus 20 μM $CuCl_2$ at 37 °C for 30 min. (B) The ^{32}P-5′-end-labeled 337-base-pair fragment (*Pst*I 2345–*Ava*I* 2681) was used. After the piperidine treatment, DNA fragments were electrophoresed, and the autoradiogram was obtained as described in Figure 6 legend. The relative amounts of oligonucleotides produced were measured by scanning the autoradiogram with a laser densitometer. Horizontal axis, the nucleotide number of human c-Ha-*ras*-1 protooncogene starting with the *Bam*HI site (Capon et al., 1983). Underscoring indicates the 12th codon of human c-Ha-*ras*-1 protooncogene.

Fe(III)–EDTA ~ heme. Iproniazid, on the other hand, caused DNA damage in the presence of Cu(II) but not in the presence of Mn(II), Mn(III), or Fe(II) (Figure 3B). Neither isoniazid nor iproniazid induced DNA damage in the presence of peroxidase/H_2O_2 at pH 7.9 (data not shown).

Isoniazid plus Cu(II)-induced DNA damage increased linearly with time (Figure 4A), whereas DNA damage by isoniazid plus Mn(II) proceeded rapidly (Figure 4B). DNA cleavage was appreciable without piperidine treatment, suggesting the breakage of deoxyribose phosphate backbone. With piperidine treatment, the damage was increased (lane 4/lane 5), indicating the involvement of base alteration and/or liberation.

The addition of bathocuproine, a Cu(I)-specific chelating agent, completely inhibited DNA damage by isoniazid plus Cu(II) (Figure 5A). DTPA also inhibited DNA damage induced by isoniazid plus Cu(II) (data not shown).

Effects of Scavengers on DNA Damage Induced by Isoniazid in the Presence of Cu(II) or Mn(II). Figure 5A shows the effects of •OH scavengers, SOD, and catalase on DNA damage induced by isoniazid plus Cu(II). Catalase (lane 7) suppressed the DNA damage, whereas •OH scavengers (lanes 2–5) and SOD (lane 6) did not. With iproniazid plus Cu(II), similar scavenger effects were observed. In contrast, DNA damage by isoniazid plus Mn(II) was inhibited by ethanol (Figure 5B, lane 2), mannitol (lane 3), sodium formate (lane 4), dimethyl sulfoxide (lane 5), and SOD (lane 6). However, the DNA damage was not inhibited by catalase (lane 7). Similar scavenger effects were observed with Mn(III) plus isoniazid (data not shown).

Site Specificity of DNA Cleavage Induced by Isoniazid or Iproniazid in the Presence of Metal Ions. To estimate the site specificity of DNA cleavage, ^{32}P-5′-end-labeled DNA fragments treated with isoniazid or iproniazid in the presence of Cu(II), Mn(II), or Mn(III) were electrophoresed, and the autoradiogram is shown in Figure 6. For the measurement of relative intensity of DNA cleavage, the autoradiograms were scanned with a laser densitometer (Figures 7 and 8). The DNA cleavage sites were determined by reference to the cleavage position produced by the procedure of Maxam and Gilbert (1980). Isoniazid plus Cu(II) induced site-specific cleavage; the predominant cleavage sites were the guanine residue of the 5′-CAG-3′ sequence and the thymine residue of the 5′-GTC-3′ sequence (Figure 7). Iproniazid plus Cu(II) showed a cleavage pattern similar to that of isoniazid plus Cu(II) (Figure 6, lanes 1 and 2). The pattern of DNA cleavage induced by isoniazid plus Cu(II) is compared with that of isoniazid plus Mn(II) (Figure 8). The DNA cleavage by isoniazid plus Mn(II) occurred at positions of every nucleotide with a little weaker cleavage at adenine residues. Similarly, isoniazid plus Mn(III) caused DNA cleavage without marked site specificity (Figure 6, lane 4).

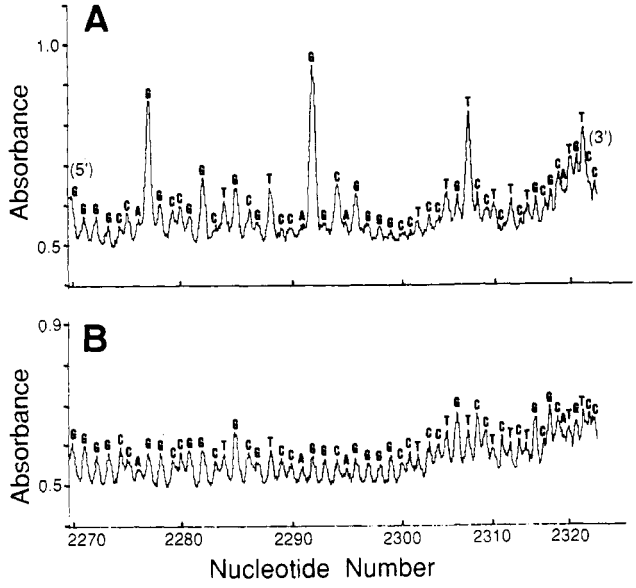

FIGURE 8: Comparison of site specificity of DNA cleavage induced by isoniazid in the presence of Cu(II) and Mn(II). (A) The ^{32}P-5'-end-labeled 98-base-pair fragment (*AvaI** 2247–*PstI* 2344) in 200 μL of 10 mM sodium phosphate buffer at pH 7.9 containing 5 μM DTPA and 20 μM per base of sonicated calf thymus DNA was incubated with 0.5 mM isoniazid plus 20 μM $CuCl_2$ at 37 °C for 30 min. (B) $MnCl_2$ was added instead of $CuCl_2$. After the piperidine treatment, DNA fragments were analyzed as described in the Figure 7 legend.

Production of •OH during Manganese-Catalyzed Autoxidation of Isoniazid. Figure 9A shows an ESR spectrum of a spin adduct observed when DMPO was added to a buffer solution containing isoniazid and Mn(II). A similar spectrum was observed with isoniazid plus Mn(III) (Figure 9F). The spin adduct ($a_N = a_H = 14.8$ G) is assigned to DMPO–OH by referring to the reported constants (Buettner, 1987). Addition of ethanol and formate resulted in the formation of the α-hydroxyethyl radical adduct of DMPO with $a_N = 16.3$ G, $a_H = 23.3$ G (Figure 9B), and $\cdot CO_2^-$ radical adduct of DMPO with $a_N = 15.7$ G, $a_H = 18.8$ G (data not shown), respectively, which are in good agreement with reported constants (Buettner, 1987). These results indicate that •OH reacts with ethanol and formate to produce α-hydroxyethyl radical and $\cdot CO_2^-$ radical, respectively. With isoniazid plus Mn(III), similar inhibitory effects of •OH scavengers were observed (Figure 9G). SOD completely inhibited the yield of DMPO–OH (Figure 9C), and catalase did not inhibit it (Figure 9E). These results show that isoniazid plus Mn(II) produced •OH via O_2^- but not via H_2O_2. In contrast, DMPO–OH was not observed during Mn(II)- or Mn(III)-catalyzed autoxidation of iproniazid. With Cu(II)-catalyzed autoxidation, neither iproniazid nor isoniazid yielded DMPO–OH.

Production of Carbon-Centered Radical Adducts during Copper-Catalyzed Autoxidation of Isoniazid and Iproniazid. Figure 10B shows an ESR spectrum of carbon-centered radical adduct observed when POBN was added to a buffer solution containing iproniazid plus Cu(II). Since the similar spectrum was not observed with isoniazid, the signals ($a_N = 15.9$ G, $a_H = 2.1$ G) can be tentatively assigned to the isopropyl radical adduct of POBN (Albano & Tomasi, 1987). The signals ($a_N = 15.4$ G, $a_H = 2.9$ G) observed with isoniazid plus Cu(II) (Figure 10A) may be assigned to adduct of POBN with isonicotinoyl (=pyridinecarbonyl) radical. Sinha (1983) suggested the formation of isonicotinoyl radical from isoniazid.

Formation of H_2O_2 during Manganese-Catalyzed Autoxidation of Hydrazines. Figure 11 shows the effect of Mn(II)

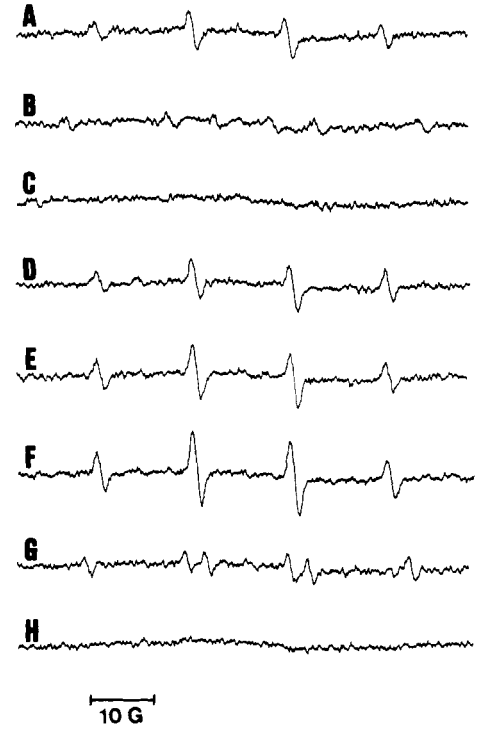

FIGURE 9: ESR spectra of the radical adducts of DMPO produced during the manganese-catalyzed autoxidation of isoniazid in the presence of various scavengers. The sample (100 μL) contained 0.5 mM isoniazid or iproniazid, 20 μM $MnCl_2$ or Mn(III)–pyrophosphate, and scavenger in 20 mM sodium phosphate buffer (pH 7.9) containing 5 μM DTPA. Spectrum A, isoniazid + Mn(II); spectrum B, isoniazid + Mn(II) + 1.6 M ethanol; spectrum C, isoniazid + Mn(II) + SOD (15 units); spectrum D, isoniazid + Mn(II) + heat-denatured SOD (15 units); spectrum E, isoniazid + Mn(II) + catalase (15 units); spectrum F, isoniazid + Mn(III); spectrum G, isoniazid + Mn(III) + 0.2 M sodium formate; spectrum H, iproniazid + Mn(II). After the addition of 14.6 mM DMPO, aliquots of the solution were immediately taken in a calibrated capillary, and ESR spectra were measured at room temperature as described under Materials and Methods.

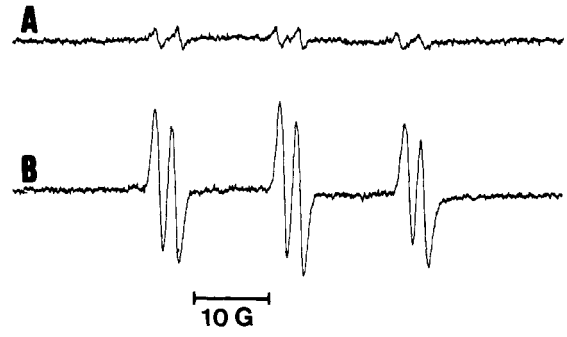

FIGURE 10: ESR spectra of the radical adduct of POBN produced from isoniazid or iproniazid in the presence of Cu(II). Spectrum A, 10 mM POBN incubated with 0.5 mM isoniazid, 20 μM $CuCl_2$, and 5 μM DTPA in 20 mM sodium phosphate buffer (pH 7.9) at 37 °C for 40 min; spectrum B, iproniazid was used instead of isoniazid, and incubation time was 20 min. ESR spectrum was measured at room temperature as described under Materials and Methods.

on the O_2 consumption during the autoxidation of isoniazid and related hydrazines. When catalase was added, the immediate increase of O_2 concentration was observed, indicating that H_2O_2 was produced during the Mn(II)-catalyzed autoxidation. However, we could not find unambiguous correlation between the cellular DNA damage and the efficiency of H_2O_2 production (as estimated by O_2 concentration rate and H_2O_2 yield). When Mn(III) was used instead of Mn(II), the autoxidation proceeded more rapidly (data not

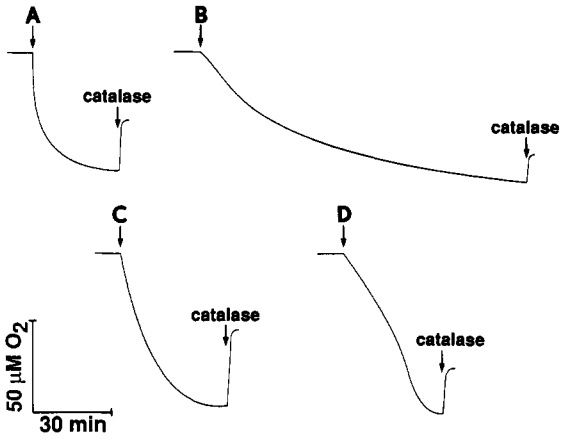

FIGURE 11: O_2 consumption and H_2O_2 production during the autoxidation of hydrazines in the presence of Mn(II). The O_2 consumption was measured in a thermostated (37 °C) water-jacketed glass vessel, fitted with a Clark electrode. Fifty micromolar isoniazid (A), iproniazid (B), hydrazine (C), or phenylhydrazine (D) was added to 1.8 mL of 50 mM sodium phosphate buffer at pH 7.9 containing 5 μM DTPA and 20 μM $MnCl_2$. After the O_2 consumption, 54 units of catalase was added.

shown). Mn(III)-catalyzed autoxidation of 50 μM hydrazine resulted in consumption of 83 μM O_2 and production of 65 μM H_2O_2.

DISCUSSION

Table I summarizes the data concerning damage to isolated and cellular DNA induced by isoniazid and related hydrazines in the presence of metal ions. Isoniazid induced cleavage of isolated DNA in combination with Cu(II), Mn(II), and Mn(III), although the cleavage did not occur with isoniazid alone. On the other hand, iproniazid caused DNA damage in the presence of Cu(II) but not in the presence of Mn(II) or Mn(III). Our previous study has shown that hydrazine damaged isolated DNA in the presence of Cu(II), Mn(II), and Mn(III) (Yamamoto & Kawanishi, 1991a). Similar results were observed with phenylhydrazine (Yamamoto & Kawanishi, 1992).

In the cellular DNA, isoniazid, hydrazine, and phenylhydrazine produced double-strand breaks in combination with Mn(II), whereas the breaks were not observed with iproniazid. Treatment with hydrazines alone did not produce the strand breaks. We have designed an experimental protocol which allows the detection of DNA single-strand breaks plus alkali-labile sites by PFGE. With alkali treatment, isoniazid, hydrazine, and phenylhydrazine were shown to produce single-strand breaks plus alkali-labile sites in DNA of Mn(II)-pretreated cells. It is well-known that single-strand breaks and/or alkali-labile regions occur spontaneously and also during synthesis of new DNA. However, it has been reported that there is an upper limit for unwinding of double-stranded DNA by treatment with alkali in the gel environment because of interaction between molecules and physical constraints (Cleaver, 1989). Consistently, under the experimental conditions employed, no effect of alkali treatment was observed with control DNA and restriction endonuclease *Not*I-treated DNA. Therefore, it seems reasonable to suppose that the increase of the level of DNA fragmentation by alkali treatment compared to that of the corresponding alkali-nontreated sample was due to single-strand breaks and alkali-labile sites introduced by DNA-damaging agents.

It is considered that •OH causes DNA cleavage at every nucleotide with no marked site specificity (Kawanishi et al., 1986; Celander & Cech, 1990). The present study shows that isoniazid plus Mn(II) causes cleavage of isolated DNA at every nucleotide with a little weaker cleavage at positions of adenine, suggesting the •OH involvement. The cleavage was inhibited by •OH scavengers and SOD but not by catalase. Consistently, in ESR spin-trapping experiment the •OH was trapped by DMPO upon the reaction of isoniazid with Mn(II). The DMPO–OH formation was inhibited by •OH scavengers and SOD, while catalase had no effect. Similar results were obtained with isoniazid plus Mn(III). On the basis of the above findings, it is considered that Mn(II) readily reacts with O_2 in the presence of isoniazid to produce Mn(III) and O_2^-, and subsequently •OH is generated to cause DNA damage. A similar mechanism could be considered with hydrazine and 1,2-dimethylhydrazine (Kawanishi & Yamamoto, 1991; Yamamoto & Kawanishi, 1991a).

The mechanism which leads to the formation of •OH and H_2O_2 during the Mn(II)-mediated autoxidation of hydrazine is likely to involve the reactions:

$$Mn^{3+} + NH_2NH_2 \rightarrow Mn^{2+}(^{\bullet}NHNH_2) + H^+ \quad (1)$$

$$Mn^{2+}(^{\bullet}NHNH_2) + O_2 \rightarrow Mn^{2+} + NH{=}NH + O_2^- + H^+ \quad (2)$$

$$Mn^{2+} + O_2^- \rightarrow MnO_2^+ \quad (3)$$

$$MnO_2^+ + NH_2NH_2 \rightarrow [MnO_2H^+] + {}^{\bullet}NHNH_2 \quad (4)$$

$$[MnO_2H^+] + H^+ \rightarrow Mn^{3+} + {}^{\bullet}OH\ (0.5H_2O_2) + OH^- \quad (5)$$

$${}^{\bullet}NHNH_2 \rightarrow 0.5NH_2NH_2 + 0.5NH{=}NH \quad (6)$$

$$1.5NH{=}NH + 1.5O_2 \rightarrow 1.5N_2 + 1.5H_2O_2 \quad (7)$$

$$1.5NH_2NH_2 + 2.5O_2 \rightarrow 1.5N_2 + 2H_2O_2 + H_2O \quad \text{(overall reaction)}$$

The amounts of production of H_2O_2 and consumption of NH_2NH_2 and O_2 agreed stoichiometrically with overall reaction. Lim and Fagg (1984) suggested the formation of $Mn^{2+}(^{\bullet}NHNH_2)$ in Mn(II)-catalyzed autoxidation of aqueous hydrazine. The formation of MnO_2^+, which has been suggested by Cabelli and Bielski (1984), appears to play an important role in the noteworthy mechanism of •OH formation not via H_2O_2.

Predominant piperidine-labile sites induced by isoniazid plus Cu(II) were found to be the guanine residue of a 5′-CAG-3′ sequence and the thymine residue of a 5′-GTC-3′ sequence. Similar sequence-specific cleavage was observed with iproniazid plus Cu(II). In a previous paper, we reported that cleavage at the thymine residues of 5′-GTC-3′ sequence induced by hydrazine plus Cu(II) was probably due to the Cu(I)–peroxide complex (Yamamoto & Kawanishi, 1991a). The inhibitory effects of bathocuproine and catalase on isoniazid plus Cu(II)-induced DNA damage indicate that a complex of Cu(I) with H_2O_2 may participate in the DNA damage, especially in the cleavage at thymine residues of the 5′-GTC-3′ sequence. The piperidine-labile guanine residue of 5′-CAG-3′ sequence, which was not observed with hydrazine plus Cu(II), may be due to the strong interaction of 5′-CAG-3′ sequence or the neighboring sequence with isoniazid or

Table I: Summary of Metal-Mediated Hydrazine-Induced DNA Damages and Mn(II)-Catalyzed Autoxidation of Hydrazines

	cellular DNA damage		isolated DNA damage			autoxidation[a]	
						initial O_2 consumption rate (μM/min)	H_2O_2 yield (μM)
added metal:	none	Mn(II)	none	Mn(II)/Mn(III)	Cu(II)	Mn(II)	
isoniazid	–	+	–	+	+	72.3	53.7
iproniazid	–	–	–	–	+	2.4	31.4
hydrazine	–	+	–	+[b]	+[b]	12.0	82.9
phenylhydrazine	–	+	–	+[c]	+[c]	2.6	46.9

[a] Fifty micromolar hydrazines were incubated with 20 μM $MnCl_2$. [b] Yamamoto and Kawanishi (1991a). [c] Yamamoto and Kawanishi (1992).

Mechanism 1

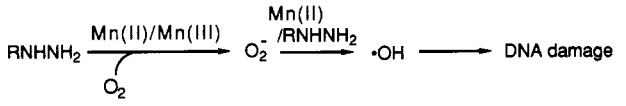

Mechanism 2

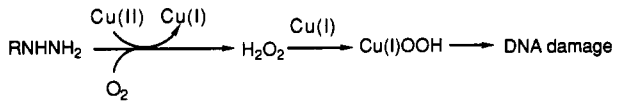

Mechanism 3

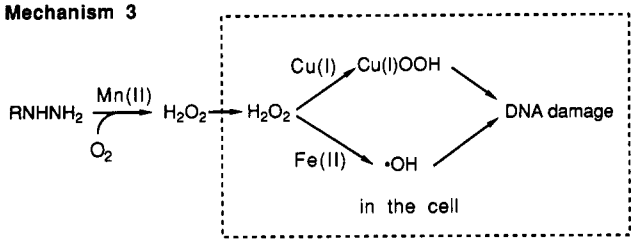

FIGURE 12: Possible mechanisms for metal-mediated DNA damage by hydrazines in vivo.

iproniazid. Relevantly, Divakar et al. (1987) have suggested the interaction of DNA with the Cu(II) complex of isoniazid. Alternatively, isonicotinoyl peroxyl radical may participate in cleavage of the guanine residue of 5′-CAG-3′ sequence since the present ESR experiment suggested the production of isonicotinoyl radical from isoniazid.

On the basis of all the above findings, we propose possible mechanisms, as shown in Figure 12, for DNA damage induced by isoniazid and related hydrazines in vivo. Mechanism 1 represents DNA damage due to •OH formed during manganese-mediated oxidation of hydrazines. Our results with isoniazid, hydrazine, and phenylhydrazine suggest that mechanism 1 is responsible, at least in part, for the hydrazine-induced oxidative DNA damage in vivo. The results with isolated DNA also suggest possible involvement of copper-mediated DNA damage via Cu(I)–peroxide complex and/or other active species in some conditions in vivo (mechanism 2). However, the role of manganese in hydrazine-induced cellular DNA damage cannot be explained by mechanism 2. Mechanism 3 represents DNA damage due to Mn(II)-mediated H_2O_2 formation; H_2O_2 generated in the cells can react with endogenous metal ions such as Fe(II) and Cu(I) bound to or close to the DNA to produce active species. This mechanism may be supported by the observation that H_2O_2 was generated during Mn(II)-catalyzed autoxidation of hydrazines. However, unambiguous correlation between the extent of the cellular DNA damage and the efficiency of H_2O_2 production was not observed. Therefore, it is considered that two or three mechanisms could proceed simultaneously. The mechanism of manganese-catalyzed •OH formation not via H_2O_2 is of particular interest in connection with the possible involvement of manganese as catalytic metal for •OH generation in vivo.

Isoniazid is one of the drugs which induce a disease with autoimmune features resembling systemic lupus erythematosus (Uetrecht, 1988). Recently, it has been suggested that active oxygen species induce antigenic changes in DNA (Blount et al., 1989). Antibodies to DNA with unusual conformation were observed in patients with systemic lupus erythematosus (Lafer et al., 1983). We previously speculated that oxidative DNA damage induced by hydralazine in the presence of either Cu(II) or peroxidase/H_2O_2 could be involved in hydralazine-induced lupus (Yamamoto & Kawanishi, 1991b). Similarly, it may be considered that isoniazid causes oxidative DNA damage through metal-mediated reaction, leading to the alteration of DNA conformation followed by the formation of anti-nuclear antibody.

ACKNOWLEDGMENT

We are grateful to Professor Masayuki Ikeda for his encouragement throughout this work.

REFERENCES

Albano, E., & Tomasi, A. (1987) *Biochem. Pharmacol. 36*, 2913–2920.

Archibald, F. S., & Fridovich, I. (1982) *Arch. Biochem. Biophys. 214*, 452–463.

Bhide, S. V., Maru, G. B., Mate, N. B., Menon, M., & Gangadharan, P. (1981) *J. Cancer Res. Clin. Oncol. 99*, 153–166.

Blöcher, D., Einspenner, M., & Zajackowski, J. (1989) *Int. J. Radiat. Biol. 56*, 437–448.

Blount, S., Griffiths, H. R., & Lunec, J. (1989) *FEBS Lett. 245*, 100–104.

Braun, R., Jäkel, H.-P., & Schöneich, J. (1984) *Mutat. Res. 137*, 61–69.

Buettner, G. R. (1987) *Free Radical Biol. Med. 3*, 259–303.

Cabelli, D. E., & Bielski, B. H. J. (1984) *J. Phys. Chem. 88*, 6291–6294.

Capon, D. J., Chen, E. Y., Levinson, A. D., Seeburg, P. H., & Goeddel, D. V. (1983) *Nature 302*, 33–37.

Celander, D. W., & Cech, T. R. (1990) *Biochemistry 29*, 1355–1361.

Cleaver, J. E. (1989) *Carcinogenesis 10*, 1691–1696.

Divakar, S., Vasudevachari, M. B., Antony, A., & Easwaran, K. R. K. (1987) *Biochemistry 26*, 3781–3785.

Gutteridge, J. M. C., Zs.-Nagy, I., Maidt, L., & Floyd, R. A. (1990) *Arch. Biochem. Biophys. 277*, 422–428.

Halliwell, B., & Aruoma, O. I. (1991) *FEBS Lett. 281*, 9–19.

Hanna, P. M., Kadiiska, M. B., & Mason, R. P. (1992) *Chem. Res. Toxicol. 5*, 109–115.

Imlay, J. A., Chin, S. M., & Linn, S. (1988) *Science 240*, 640–642.
Inoue, S., & Kawanishi, S. (1987) *Cancer Res. 47*, 6522–6527.
Inoue, S., & Kawanishi, S. (1989) *Biochem. Biophys. Res. Commun. 159*, 445–451.
Kawanishi, S., & Yamamoto, K. (1991) *Biochemistry 30*, 3069–3075.
Kawanishi, S., Inoue, S., & Sano, S. (1986) *J. Biol. Chem. 261*, 5952–5958.
Lafer, E. M., Valle, R. P. C., Möller, A., Nordheim, A., Schur, P. H., Rich, A., and Stollar, B. D. (1983) *J. Clin. Invest. 71*, 314–321.
Lim, P. K., & Fagg, B. S. (1984) *J. Phys. Chem. 88*, 1136–1140.
Liochev, S. I., & Fridovich, I. (1991) *Arch. Biochem. Biophys. 291*, 379–382.
Loeb, L. A., James, E. A., Waltersdorph, A. M., & Klebanoff, S. J. (1988) *Proc. Natl. Acad. Sci. U.S.A. 85*, 3918–3922.
MacRae, W. D., & Stich, H. F. (1979) *Mutat. Res. 68*, 351–365.
Maru, G. B., & Bhide, S. V. (1982) *Cancer Lett. 17*, 75–80.
Maxam, A. M., & Gilbert, W. (1980) *Methods Enzymol. 65*, 499–560.
Mello-Filho, A. C., & Meneghini, R. (1991) *Mutat. Res. 251*, 109–113.
Parodi, S., De Flora, S., Cavanna, M., Pino, A., Robbiano, L., Bennicelli, C., & Brambilla, G. (1981) *Cancer Res. 41*, 1469–1482.
Severi, L., & Biancifiori, C. (1968) *J. Natl. Cancer Inst. 41*, 331–340.
Shibutani, S., Takeshita, M., & Grollman, A. P. (1991) *Nature 349*, 431–434.
Sinha, B. K. (1983) *J. Biol. Chem. 258*, 796–801.
Stadtman, E. R., & Berlett, B. S. (1991) *J. Biol. Chem. 266*, 17201–17211.
Tkeshelashvili, L. K., McBride, T., Spence, K., & Loeb, L. A. (1991) *J. Biol. Chem. 266*, 6401–6406.
Toth, B. (1975) *Cancer Res. 35*, 3693–3697.
Toth, B., & Shubik, P. (1966) *Cancer Res. 26*, 1473–1475.
Uetrecht, J. P. (1988) *Chem. Res. Toxicol. 1*, 133–143.
Wade, D. R., Lohman, P. H. M., Mattern, I. E., & Berends, F. (1981) *Mutat. Res. 89*, 9–20.
Whiting, R. F., Wei, L., & Stich, H. F. (1979) *Mutat. Res. 62*, 505–515.
Whiting, R. F., Wei, L., & Stich, H. F. (1980) *Biochem. Pharmacol. 29*, 842–845.
Yamamoto, K., & Kawanishi, S. (1989) *J. Biol. Chem. 264*, 15435–15440.
Yamamoto, K., & Kawanishi, S. (1991a) *J. Biol. Chem. 266*, 1509–1515.
Yamamoto, K., & Kawanishi, S. (1991b) *Biochem. Pharmacol. 41*, 905–914.
Yamamoto, K., & Kawanishi, S. (1992) *Chem. Res. Toxicol. 5*, 440–446.
Yamamoto, K., Inoue, S., Yamazaki, A., Yoshinaga, T., & Kawanishi, S. (1989) *Chem. Res. Toxicol. 2*, 234–239.
Yamazaki, I., & Piette, L. H. (1991) *J. Am. Chem. Soc. 113*, 7588–7593.
Yim, M. B., Berlett, B. S., Chock, P. B., & Stadtman, E. R. (1990) *Proc. Natl. Acad. Sci. U.S.A. 87*, 394–398.
Zetterberg, G., & Boström, G. (1981) *Mutat. Res. 91*, 215–219.